Time dependence of ionization and excitation by few-cycle laser pulses

Darko Dimitrovski* and Lars Bojer Madsen
Lundbeck Foundation Theoretical Center for Quantum Systems Research, Department of Physics and Astronomy, University of Aarhus, 8000 Aarhus C, Denmark
(Received 8 September 2008; published 31 October 2008)

We investigate theoretically the time dependence of few-cycle strong-field ionization and excitation in an attosecond-femtosecond–pump-probe scenario. We demonstrate that a combination of simple techniques, relying on perturbation and tunneling theory, are very useful for the description of electron dynamics during the time evolution. Our studies show that half-cycle ionization dynamics is responsible for the difference of the rise time in the ionization steps from the tunneling steps and for the appearance of dips in the ionization probability time dependence.

DOI: 10.1103/PhysRevA.78.043424 PACS number(s): 32.80.Rm, 42.50.Hz

I. INTRODUCTION

Attosecond pulses can be generated in the extreme ultraviolet (xuv) using high-harmonic generation induced by a few-cycle near-infrared (near-ir) femtosecond (fs) pulse [1–3]. The pulses are synchronized, and by varying the time delay between them and using the xuv pulse to initiate or terminate dynamics in the fs field, the dynamics of the continuum electron can be monitored [4–6]. In the experiment [5], for example, an xuv attosecond pulse was used to produce Ne^+ ions in an excited state. A near-ir fs pulse too weak to ionize Ne from the ground state but strong enough to ionize Ne^+ from the excited state was applied with a time delay. By measuring the yield of Ne^{2+} ions as a function of the delay between the xuv and near-ir pulses, the time dependence of ionization, which is a steplike structure preceded by dips, was reconstructed. The results were interpreted using the nonadiabatic tunnel ionization theory [7], which fitted the results reasonably well. The steepness of the steps and the occurrence of the dips, however, were not reproduced by the tunneling model. The dips were thought to arise from the electron-electron interaction [5]. The question on the origin of these dips and the steepness of the steps is presently open [8], although some light has been shed on the problem in a very recent paper [9]. This question is closely related to the general theoretical question of the time dependence of ionization and excitation, which, in the view of the availability of the attosecond-femtosecond pump-probe experiments, ceases to be an academic question [10]. Here we address this question by performing a theoretical analysis of the time dependence of ionization and excitation probability. Our approach to a description of the time dependence of ionization and excitation differs from the one in Refs. [11,12] in two important ways. First, instead of building up a relatively complicated theoretical framework, we show the usefulness of simple perturbation and tunneling theories—in particular, the lowest-order time-dependent perturbation theory turns out to be very useful. Second, we adopt and exploit the results obtained by analysis of half-cycle pulses—in particular, the transition from the short-time to the adiabatic limit [13,14]. We show that the results of xuv-pump–near-ir probe experiments can be interpreted in terms of a transition from the short-pulse to the adiabatic limit for each half-cycle of the field. In addition, we explicitly show the transition from the time-dependent field description to the photon-based description [15] *during* the time evolution of the pulse.

The paper is organized as follows. In the next section we discuss the switch-on (switch-off) scenarios corresponding effectively from the atomic system's point of view to a sudden turn-on (turn-off) of the near-ir fs field by the attosecond pump. In Sec. III, we formulate the basic analytic approximations used in the analysis. The main features of the ionization time dependence for a few-cycle laser pulse are discussed in Sec. IV. In Sec. V, we perform detailed analysis in cases of half- and one-cycle pulses and for ionization processes starting from different excited states, including a coherent superposition, with the aim to investigate the origin of the structures in the time dependence of ionization. Conclusions are given in Sec. VI. Atomic units $[\hbar = m_e = |e| = 1]$ are used throughout unless indicated otherwise.

II. SWITCH-ON, SWITCH-OFF SCENARIOS

We consider two ways to "record" the ionization probability $P_{\mathrm{ion}}(\Delta t)$ as a function of time Δt available for ionization in the near-ir fs field. In the first type, which was realized experimentally [5], an attosecond xuv pulse excites an electron from an inner shell. Subsequently, a near-ir fs pulse ejects this electron into the continuum. Under the assumption that the electron is instantly excited by the xuv pulse, the time dependence of $P_{\mathrm{ion}}(\Delta t)$ is monitored by varying the time delay between the center of the pulses. This procedure formally amounts to a response to a field with the shape depicted in Fig. 1(a): the pulse is suddenly switched on at a particular instant of time and effectively leaves the system to ionize for a time Δt. In the second scenario which was discussed theoretically [8], the xuv pulse promotes an inner-shell electron to the continuum. Then the electron in the outer shell suddenly "feels" the attractive force of the nucleus and the process of strong near-ir ionization is stopped. By adjusting the delay between the xuv and near-ir pulses, the ionization caused by the near-ir pulse can be ef-

*darkod@phys.au.dk

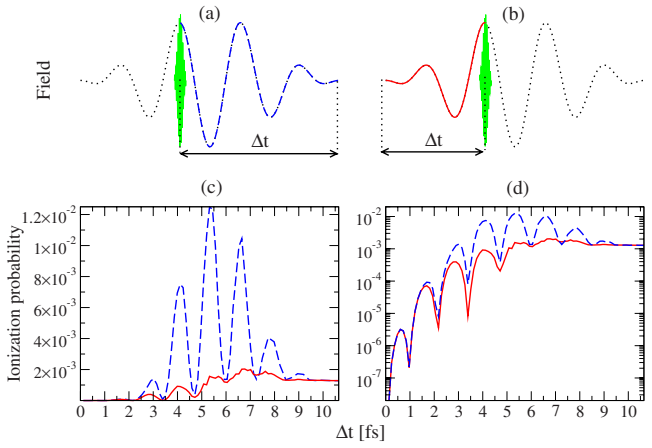

FIG. 1. (Color online) Types of attosecond-pump–femtosecond-probe experiments: (a) switch-on and (b) switch-off of the near-ir pulse caused by the action of an attosecond xuv pulse. The shaded bursts illustrate the xuv pulse. (c) Comparison of the time dependence of ionization of H(1*s*) in the switch-on (long-dashed curve) and switch-off (solid curve) scenarios on linear and (d) logarithmic scales. The parameters are 800 nm, 7×10^{13} W/cm^2, and the duration is 10 fs.

fectively switched off at a particular instant of time [Fig. 1(b)].

These two types of pump-probe experiments yield very different results, even for atoms with a single active electron. We illustrate this in Figs. 1(c) and 1(d) by the results of *ab initio* calculations for $P_{\rm ion}(\Delta t)$ for H(1*s*) in the field detailed in the caption. The time dependence of ionization was obtained by propagating the time-dependent Schrödinger equation (TDSE) in the dipole approximation and projecting the wave function onto discretized field-free continuum states during the pulse using two different approaches. First, we solved the TDSE in the length gauge based on the discrete variable representation (DVR) of state vectors in parabolic coordinates [16]. Second, we used a grid method [17] in both length and velocity gauges [10]. The results for $P_{\rm ion}(\Delta t)$ obtained from the two methods agree excellently. In the subsequent calculations, we have used the DVR code only.

From the curves of the time dependence of $P_{\rm ion}(\Delta t)$ in Figs. 1(c) and 1(d), we note the absence of strict tunneling steps [5] in the time dependence of ionization and the existence of dips even in the case of a switch-off type of pulse. Furthermore, the amplitude of the oscillation is much larger in the case of switch-on than switch-off, reflecting the fact that the sudden switch-on of the field causes excitation of the atom and the process of ionization begins from a coherent superposition of states. That can be explained as follows. Let us restrict ourselves to the independent-electron model and take into account only the electron which is conditionally sensitive to the action of the xuv pulse. Then modeling of both switch-on and switch-off scenarios reduces to the introduction of a time-dependent atomic potential, which suddenly changes upon arrival of the xuv pulse from a potential with larger attraction to a potential with less attraction (switch-on case) and vice versa (switch-off case) [9]. Since the sudden switch-on adds an additional level of complexity, in the following, we concentrate on the switch-off type of experiments and analyze the corresponding time dependence. To isolate the main effects and to obtain theoretically tractable results, we consider the instantaneous switch-off dynamics for H(1*s*). We have checked that the results are insignificantly influenced by convoluting $P_{\rm ion}(\Delta t)$ with the intensity profile of the xuv pulse used also in [5], to account for the influence of the attosecond pulse.

III. THEORY

In order to investigate the time dependence of ionization we consider two simple approximations valid in different time and intensity regimes: the first-order time-dependent perturbation theory (FPT) and tunneling. In addition to the above approximations, we will also consider the strong-field approximation (SFA) [18,19], which has become a standard theoretical tool for a description of ionization by strong femtosecond pulses. All approximations will be derived in length gauge, allowing directly for the correct description of the time dependence of ionization and excitation [10].

A. First-order time-dependent perturbation theory

The transition amplitude as a function of time in FPT is for a field $\mathbf{F}(t)=F(t)\hat{z}$,

$$a_{f,i}(\Delta t) = -i\langle\phi_f|z|\phi_i\rangle\int_{-\infty}^{\Delta t} F(t)\exp(i\Delta E t)dt, \tag{1}$$

where $\langle\phi_f|z|\phi_i\rangle$ is the dipole matrix element between the initial state ϕ_i with energy E_i and final state ϕ_f with energy E_f, and $\Delta E=E_f-E_i$. The dipole matrix elements between the ground state and an excited $\phi_{n,l,m}$ or a continuum state ϕ_{Elm} are known for hydrogenic systems (see, e.g., [20]). For example, the dipole matrix element between the ground state $\phi_i\equiv\phi_{1s}$ and a continuum state ϕ_{Elm} of energy E and orbital and magnetic quantum numbers l and m is nonzero for $l=1$ and $m=0$ only and is given by

$$\langle\phi_{E10}|z|\phi_i\rangle = \frac{2^4\exp\left(-\frac{2}{\sqrt{2E}}\arctan\sqrt{2E}\right)}{(1+2E)^{5/2}\sqrt{3\left(1-\exp\left(-\frac{2\pi}{\sqrt{2E}}\right)\right)}}, \tag{2}$$

and the dipole matrix element for the 1*s*-2*p* transition is

$$\langle\phi_{2p}|z|\phi_i\rangle = \frac{2^7\sqrt{2}}{3^5}. \tag{3}$$

Knowing the field $\mathbf{F}(t)$ and inserting the dipole matrix elements into Eq. (1) it is straightforward to evaluate the excitation probability time dependence. The time dependence of ionization in FPT is

$$P_{\rm ion}^{\rm FPT}(\Delta t) = \int_0^\infty dE|a_{E,i}(\Delta t)|^2, \tag{4}$$

where the contributions from all the continuum states are integrated up.

B. Strong-field approximation

The transition amplitude in the SFA [18] from a certain initial state to a continuum state of asymptotic momentum **k** is

$$a_{\mathbf{k},i}^{\mathrm{SFA}}(\Delta t) = -i\int_{-\infty}^{\Delta t} dt\langle \mathbf{k}+\mathbf{A}(t)-\mathbf{A}(\Delta t)|\mathbf{F}(t)\cdot\mathbf{r}|\phi_i\rangle \exp[iS(t)], \tag{5}$$

where $\mathbf{A}(t)=-\int_{-\infty}^{t}dt'\mathbf{F}(t')$ is the vector potential, ϕ_i is the initial state, and $\langle \mathbf{r}|\mathbf{p}\rangle = 1/(2\pi)^{3/2}\exp(i\mathbf{p}\cdot\mathbf{r})$ is a plane wave. The phase $S(t)$ that appears in Eq. (5) is given by

$$S(t) = -\int_{-\infty}^{t} dt'[E_i - E_f(t')], \tag{6}$$

where E_i is the initial binding energy and where

$$E_f(t') = \frac{1}{2}[\mathbf{k}+\mathbf{A}(t')-\mathbf{A}(\Delta t)]^2 \tag{7}$$

is the instantaneous energy of the final state. The dipole matrix element between the ground state of the hydrogen atom ϕ_i and the plane wave $\langle \mathbf{r}|\mathbf{p}\rangle$ is explicitly

$$\langle \mathbf{p}|\mathbf{F}(t)\cdot\mathbf{r}|\phi_i\rangle = -i\frac{2^{7/2}}{\pi}\frac{\mathbf{p}\cdot\mathbf{F}(t)}{(1+p^2)^3}. \tag{8}$$

The ionization probability time dependence in the SFA can be obtained as

$$P_{\mathrm{ion}}^{\mathrm{SFA}}(\Delta t) = \int d^3\mathbf{k}|a_{\mathbf{k},i}^{\mathrm{SFA}}(\Delta t)|^2. \tag{9}$$

The appearance of the vector potential $\mathbf{A}(\Delta t)$ in Eqs. (5) and (7) enables a correct treatment of the ionization time dependence. Namely, with the correction of adding $\mathbf{A}(\Delta t)$ the Volkov state goes over into a plane wave at the end of the interaction (at time instant $t=\Delta t$) [21]. We note that, since plane waves are taken as final states, the uncorrected version of the SFA with respect to the time dependence [without $\mathbf{A}(\Delta t)$] leads to the correct result for the total ionization probability time dependence; however, the time-dependent momentum distributions will be shifted by $\mathbf{A}(\Delta t)$ with respect to the momentum distribution of Eq. (5).

C. Tunneling

Tunneling is the dominant process in the adiabatic limit. The zeroth order of the adiabatic approximation for the occupation of an initial state reduces to the familiar expression for the probability of depletion of the initial state due to tunneling [16]. With the additional assumption that everything that goes out of the initial state finishes in the continuum, the tunneling ionization probability as a function of time is

$$P_{\mathrm{ion}}^{\mathrm{tun}}(\Delta t) = 1 - \exp\left(-\int_{-\infty}^{\Delta t}\Gamma_i(F(t))dt\right), \tag{10}$$

where Γ_i is the tunneling width of the initial state. For not too high fields and taking H(1*s*) as the initial state, it is accurate to use the conventional analytical tunneling formula (see, e.g., [22])

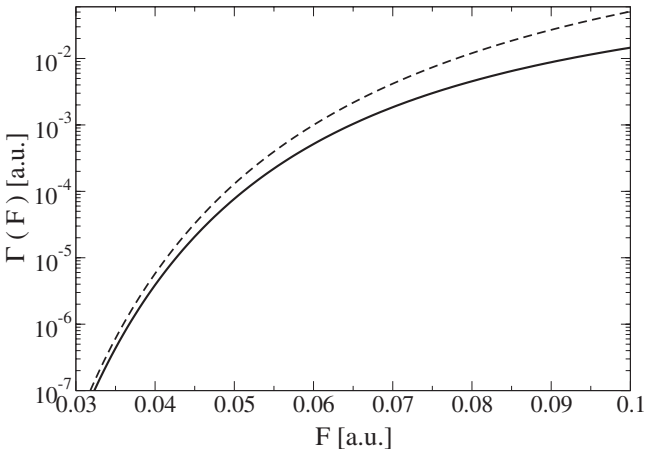

FIG. 2. Tunneling width Γ for the ground state of hydrogen as a function of field strength *F*. Solid line: tunneling width obtained in the quasistationary-state approach (12) Dashed line: tunneling width of Eq. (11).

$$\Gamma(F) = \frac{4}{F}\exp[-2/(3F)], \tag{11}$$

which is widely used. Another approach to calculate the tunneling width of the initial state is the quasistationary-state approach [23]. The eigenenergies of the quasistationary states are *discrete* and *complex*. The tunneling width of the initial state is then

$$\Gamma_i(F) = |2\ \mathrm{Im}\ E_i(F)|, \tag{12}$$

where $E_i(F)$ is the complex eigenenergy of the quasistationary state which in the limit $F\to 0$ reduces to the field-free initial state with eigenenergy E_i. The tunneling width of Eq. (12) can be calculated numerically using an approach developed in Ref. [24].

In the limit $F\to 0$, Eqs. (11) and (12) give identical results. The difference between the above tunneling widths for the ground state of hydrogen is given in Fig. 2. The difference becomes appreciable at approximately $F\sim 0.05$ a.u. (peak laser intensity $\sim 8.8\times 10^{13}$ W/cm^2). For laser pulses with larger amplitude, expression (11) *overestimates* the depletion of the initial state, thus resulting in a larger tunneling probability. Note that the tunneling width obtained in the quasistationary-state approach treats both the "under the barrier" and "over the barrier" tunneling on equal footing. Therefore, even in the barrier-suppression regime [25], the use of the tunneling width of Eq. (12) describes correctly the ionization process [13]. In cases of half-cycle pulses, it is straightforward to apply the tunneling formula of Eq. (10). In the case of few-cycle pulses we also apply Eq. (10) by replacing $F(t)$ with $|F(t)|$. We note that such an expression does not allow for a decrease of the ionization probability as a function of time.

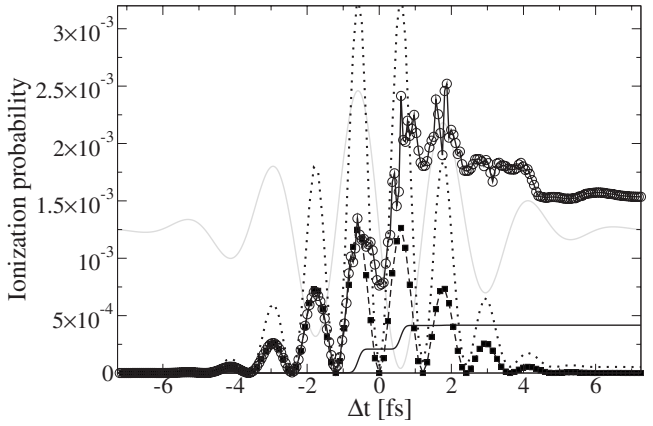

FIG. 3. Time dependence of ionization probability of H(1*s*) by a 740-nm Gaussian pulse with 5.5 fs FWHM and peak electric field of $F_0=0.045$ a.u. $(7.1\times10^{13}\ \mathrm{W/cm^2})$. The TDSE results (open circles, solid line) are compared with tunneling theory (solid line), SFA (dotted line), and FPT (solid squares, dashed line). The gray line is the electric field in arbitrary units.

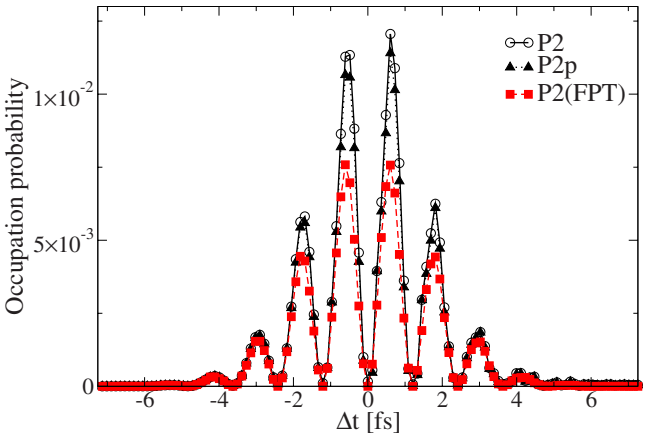

FIG. 4. (Color online) Time dependence of occupation probability of the second shell (i.e., 2*s* and 2*p* states) in H (denoted *P*2) and H(2*p*) (denoted *P*2*p*) compared to FPT [denoted *P*2(FPT)]. Pulse parameters as in Fig. 3.

IV. FEW-CYCLE PULSES

We are now ready to study in detail $P_{\mathrm{ion}}(\Delta t)$ in the switch-off case [Fig. 1(b)]. We use the pulse considered in a recent experiment [5],

$$F(t) = F_0 \exp(-t^2 4 \ln 2/\tau_{\mathrm{FWHM}}^2)\sin(\omega t), \qquad (13)$$

with parameters given in the caption of Fig. 3. The TDSE was propagated from −7.25 fs to 7.25 fs, and in Fig. 3 we compare $P_{\mathrm{ion}}(\Delta t)$ from the TDSE with $P_{\mathrm{ion}}^{\mathrm{FPT}}(\Delta t)$ of Eq. (4), $P_{\mathrm{ion}}^{\mathrm{SFA}}(\Delta t)$ of Eq. (9), and $P_{\mathrm{ion}}^{\mathrm{tun}}(\Delta t)$ of Eq. (10). By comparing the probability with the temporal variation of the field, we see clear oscillations in the ionization probability time dependence following the oscillations of the electric field of the pulse, in particular in the first part of the pulse. The tunneling theory fails to predict the numerical results for an obvious reason: while $P_{\mathrm{ion}}^{\mathrm{tun}}(\Delta t)$ exhibits sharp steps for each half–cycle of the field, the steepness of the rise in $P_{\mathrm{ion}}(\Delta t)$ in the TDSE results is not so large and the rise is followed by a dip. On the other hand, FPT is very accurate for the first ~5 half–cycles, up to the middle of the pulse. The SFA curve is qualitatively similar to the FPT curve—it follows the field oscillations, but overestimates the numerical result. We will return to the SFA in the next section.

In order to check the validity of FPT further, we consider the time dependence of excitation probability $P_{\mathrm{exc}}(\Delta t)$ during the pulse. In Fig. 4 we compare $P_{\mathrm{exc}}(\Delta t)$ of the second shell in H with the result of FPT, denoted as *P*2(FPT) in Fig. 4. Compared with the results for $P_{\mathrm{ion}}(\Delta t)$, the validity of FPT extends to later times for excitation. It appears that this improvement is due to the smaller energy separation of the 2*p* state from the 1*s* ground state compared to the separation from 1*s* and to the continuum. We have checked that this trend is satisfied for $P_{\mathrm{exc}}(\Delta t)$ also for the higher-lying bound states. Therefore, in addition to explaining $P_{\mathrm{ion}}(\Delta t)$ in the initial stages of the pulse, FPT even more accurately explains the time dependence of the excitation probability and hence offers a unique and simple tool for the analysis of attosecond time-resolved bound-state electron dynamics.

In Fig. 5 the ionization time dependence by a pulse is compared to the ionization caused by the action of *isolated* half-cycles of which the pulse itself is composed. It can be seen that up to the middle of the pulse the time dependence of the ionization is almost identical. Physically what happens in the first part of the pulse is that the ionization (and excitation) is so small that all population driven away from the 1*s* ground state by the first half of each half-cycle is driven back by the second half. As time proceeds during the pulse, a larger part of the population is moved to higher excited states and the continuum and the electron charge density can no longer adjust to the instantaneous value of the external field. However, it clearly makes sense to investigate the time dependence of ionization caused by isolated half-cycles of the field in an attempt to provide an answer to the ionization

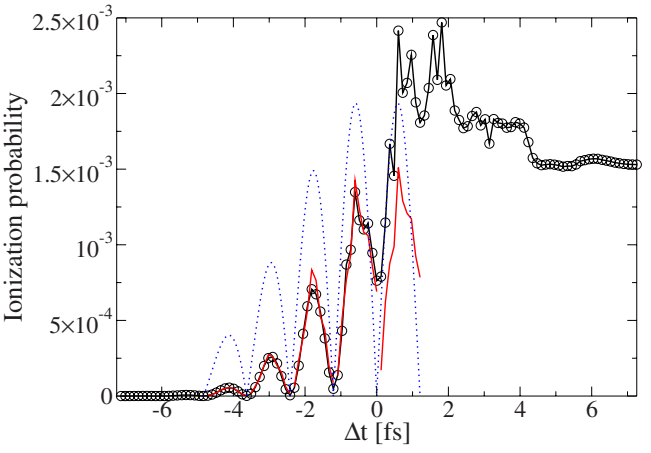

FIG. 5. (Color online) Explicit signatures of half-cycle ionization: comparision of the ionization time dependence of Fig. 3 (solid line with open circles) and ionization time dependence by the first few *isolated* half-cycles from which the pulse is assembled (solid line). The dotted line depicts the absolute value of half-cycles of the field in arbitrary units. Pulse parameters as in Fig. 3.

time dependence by a few-cycle pulse. We will study in detail this subcycle dynamics in the next section.

Turning back to the time dependence of $P_{\mathrm{ion}}(\Delta t)$ in Fig. 3, at $t \simeq 0$, $P_{\mathrm{ion}}(\Delta t)$ ceases to increase in steps and, after some oscillation, settles at a final value. We have investigated numerically the origin of this behavior by looking at the population of the bound states and found that at the end of the pulse the dominant mechanism is multiphoton ionization. For the pulse parameters of Fig. 3, we have identified that at the end of the pulse most of the excited-state population is located in the fifth and sixth shell. Taking into account the ponderomotive shift of the ionization threshold $F^2/4\omega^2$, the nine-photon absorption peaks exactly between the ac Stark-shifted states of the fifth and sixth shells. In fact, as the pulse duration increases, the full width at half maximum (FWHM) of the pulse in frequency space decreases and, at $t=7.51$ fs, becomes approximately 0.02 a.u., which is 3 times smaller than the central frequency of the pulse. Therefore the photon picture becomes appropriate and multiphoton ionization and excitation set in. Hence, we have identified a "short-time" regime, where half-cycle ionization dynamics dominates and where the time dependence is described by FPT, and a "long-time" regime, where the "normal" multiphoton ionization picture becomes appropriate. Roughly, the transition from these two regimes happens at the middle of the pulse.

V. HALF- AND ONE-CYCLE ANALYSIS: TRANSITION FROM THE SHORT-TIME TO THE ADIABATIC LIMIT

We now turn to a more detailed investigation of the origin of the dips most pronounced in the short-time limit by calculating the response of the pulse to a one-cycle pulse as given in the caption of Fig. 6. Clearly, in the limit where FTP is accurate, the dips are fully accounted for by the time dependence of the field within each half-cycle. The question we address now is to what extent an increase in intensity affects the dips and the accuracy of FPT versus tunneling theory. In Fig. 6 we present the results of TDSE calculations on H starting from the H($1s$) initial state and compare with FPT of Eqs. (1)–(4) and the tunneling expression of Eq. (10) with the quasistationary width (12).

At relatively low peak amplitude [Fig. 6(a)] corresponding to approximately 1.4×10^{13} W/cm^2, $P_{\mathrm{ion}}(\Delta t)$ follows the shape of the field: it attains its extrema at the extrema of the absolute value of the field $|F(t)|$. FPT is very close to the TDSE result, while the tunneling probability is negligible on the scale of the plot. Therefore, for the intensity in question, the ionization probability closely follows the short-time asymptote and the ionization is clearly not in the tunneling regime.

At a peak amplitude of the field of $F_0=0.045$ a.u. [Fig. 6(b), peak laser intensity of 7.1×10^{13} W/cm^2] the FPT describes correctly $P_{\mathrm{ion}}(\Delta t)$ midway through the first half-cycle, up to the first field maximum. However, $P_{\mathrm{ion}}(\Delta t)$ cannot be described by tunneling either. Not only is the absolute scale wrong, but more importantly, the shape of the time dependence is different: while the tunneling occurs in sharp steps for each half-cycle of the field, the TDSE result exhibits a rise whose steepness differs from the rise in tunneling steps and a subsequent fall (dip) which precedes the rise belonging to the next half-cycle. In this intermediate regime no simple model is able to reproduce the ionization time dependence and we have to rely on the full numerical solution of the TDSE.

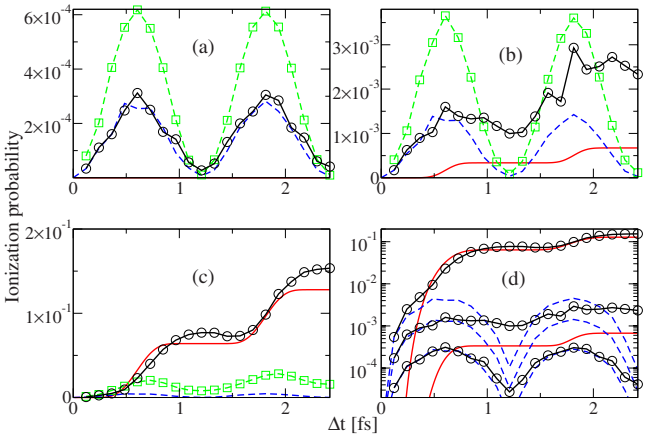

FIG. 6. (Color online) Time dependence of ionization probability for a one-cycle pulse $\boldsymbol{F}(t)=F_0 \sin(\frac{\pi t}{\tau})\hat{\boldsymbol{z}}$, $0 \leqslant t \leqslant 2\tau$, where τ is the half-cycle duration. TDSE (solid lines, open circles), FPT (dashed lines), SFA (dashed lines, open squares), and tunneling (solid line). (a) 1.4×10^{13} W/cm^2, (b) 7.1×10^{13} W/cm^2, and (c) 2.24×10^{14} W/cm^2. The logarithmic plots of (a)–(c) are given in (d). Solid lines with circles are the TDSE results, solid curves show tunneling, and dashed lines show perturbation theory. The tunneling curve for the case (a) is missing in graph (d), because it lies almost ten orders of magnitude below the exact results.

Increasing the electric field further [Fig. 6(c)], it appears that the tunneling probability approaches the exact result and hence that in the high-intensity regime time-dependent tunneling is valid for an analytical description of the time dependence of ionization. We will return to this point later and show that this is in fact not the case.

From Figs. 6(a)–6(c) it is also clear that the SFA of Eq. (5) fails to reproduce the curves of the time dependence of ionization for any intensity. This comes as no surprise, since it has been known that the most simple version of the SFA compares poorly to the exact numerical results in cases of real atoms [26]. This is in accordance with the findings in Ref. [11], where the time dependence of ionization has been compared with exact numerical results, albeit for the case of a one-dimensional soft-core potential. The discrepancy in our three-dimensional case between the SFA and the numerical results appears to be larger here than in that study. We note, however, that the most simple version of the SFA, Eq. (5), compares excellently with the numerical results in the case of the zero-range potential [14].

Figure 6(d) summarizes the results on a logarithmic scale. The tunneling curve approaches the exact numerical solution when the peak electric field is increased. At the same time, even in the case of the highest peak electric field, FPT seems appropriate in the initial stages of the pulse. These features enable an interpretation of the time dependence of ionization and excitation during a single half-cycle of the field in light of the result of Ref. [13] as a time-dependent transition from

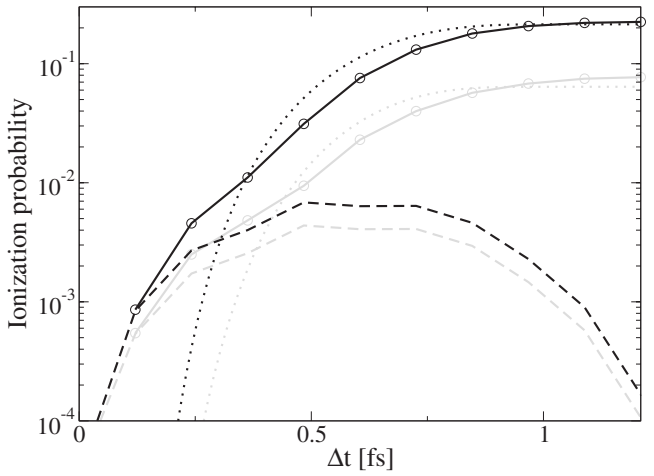

FIG. 7. Time dependence of ionization probability for a half-cycle pulse $\boldsymbol{F}(t)=F_0 \sin(\frac{\pi t}{\tau})\hat{\mathbf{z}}$, $0 \leqslant t \leqslant \tau$. TDSE (solid lines, open circles), FPT (dashed lines), and tunneling (dotted line). The curves for the peak field amplitude $F_0=0.08$ a.u. (peak intensity 2.24×10^{14} W/cm^2) are plotted in gray, while for peak field amplitude $F_0=0.1$ a.u. (peak intensity 3.51×10^{14} W/cm^2) the curves are plotted in black.

the short-pulse to the adiabatic limit. There is, however, a difference between the half-cycles used in that study and the ones used here. In the former, Gaussian-shape half–cycles were used and their peak amplitude was constant while the duration was increased. Only the result at the end of the half-cycle pulse was considered. Here, by projecting the wave function at particular instants during the time evolution of the pulse, both the amplitude and the duration of the pulse increase. However, as we will see below, the conclusions derived in [13] apply in the present study also.

In the initial stages of the pulse FPT is valid even in the cases where tunneling theory approaches the exact result [the first ~0.24 fs in Fig. 6(c) and the uppermost curve in Fig. 6(d)]. So the initial rise in the ionization probability is always reproduced by FPT. This is exactly the short-time limit discussed in [13]. Therefore, in a single half-cycle of the field, the recorded $P_{\text{ion}}(\Delta t)$, depending on the intensity, is produced by competition of two mechanisms: the FPT, valid in the short-time limit, and the tunneling probability, valid in the adiabatic limit. According to Ref. [13], the transition between these two regimes is more rapid when the peak amplitude of the pulse is larger. In the current situation, the 50 a.u. of half-cycle duration at a binding energy of 0.5 a.u. is insufficient to observe a full transition from the short-time ionization mechanism to the adiabatic regime for the intensities used in Figs. 6(a) and 6(b). At a lower intensity FPT is valid for longer times during the half-cycle, but the adiabatic regime is not attained. Only at the intensity in Fig. 6(c) is the TDSE result very close to the adiabatic result. In Fig. 7, where the half-cycle ionization time dependence is shown for peak electric fields 0.08 and 0.1 a.u., a complete transition from the short-pulse to the adiabatic limit is visible. For very short times, FPT correctly reproduces the ionization probability irrespective of intensity. On the other hand, the ionization probability at the end of the half-cycle is correctly reproduced by the tunneling formula. However, as is clearly visible from Fig. 7, this does not mean that the steepness of the time dependence of ionization can be reproduced by the tunneling formula, simply because the adiabatic approximation is invalid at shorter times.

The above analysis was carried out only for a half-cycle of the field. The question that naturally arises is whether one can continue the half-cycle analysis for the subsequent half-cycles of the field. For weak fields and not too many cycles of the field, the answer is yes. Below we explain why in detail. From Figs. 6(a) and 6(b) one sees that in the second half-cycle of the field essentially the same processes take place as in the first half-cycle. In fact, the process of ionization is continued from the point it was left at the end of the first half cycle, i.e., no appreciable recombination from the continuum to the bound states occurs. More precisely, $P_{\text{ion}}(\Delta t)$ for the second half-cycle can be approximately obtained from the first, shifted by the amount of ionization at the end of the first half-cycle. Then the conclusions which were derived for $P_{\text{ion}}(\Delta t)$ for the first half-cycle of the field apply to the second half-cycle also [14]. As long as the ionization probability follows the field oscillations and the dips occur at zero field, it is possible to use the half-cycle analysis for each subsequent half-cycle of the field. Such an approach breaks down for two reasons. In the weak-field case, by adding few half-cycles one after the other, the width of the pulse in frequency space decreases so the time-dependent-based description breaks down and the photon-based description becomes appropriate (see Fig. 3 and the discussion in the previous section). The other reason for the breakdown of such an approach is significant ionization, as in Fig. 6(c). It can be seen that the time dependence of ionization exhibits a soft "dip," which is shifted from the instant of time at which the field is zero. This happens because significant emission occurs also when the field is not at its maximum, thus creating low-energy electrons, which then in the subsequent half-cycle of the field recombine back.

In Fig. 8 we compare the time dependence of the ionization probability during one cycle of the field for different initial states of hydrogen ($1s$, $2p$, and $2s$). In all cases significant ionization occurs and there is a dip which does not correlate with the zero-field point, but occurs later in time. This dip is visible in all three curves and appears to be larger in cases with larger ionization during the first half-cycle. The dip for the case of the $1s$ initial state (these results are multiplied by 2) is smaller than the corresponding dips for $2s$ and $2p$ initial states. However, as can be seen from the differences of the dips in the cases of $2s$ and $2p$, their position and depth depend also on the symmetry of the initial state.

We have investigated more closely the instant of time when the dips occur with respect to the time dependence of the probability of occupation of the ground state and other bound states in the atom. It turns out that in the second half-cycle, the population recombines into excited states with smaller binding energy than the initial state. It appears that there is no simple model to account for the recombination to the excited states. A correct line of model development was followed in [11] where it was pointed out that the existence of the excited states enhances the electron emission into the continuum, so that the electron can escape not only directly "under" or "over" the barrier, but also through nonadiabatic

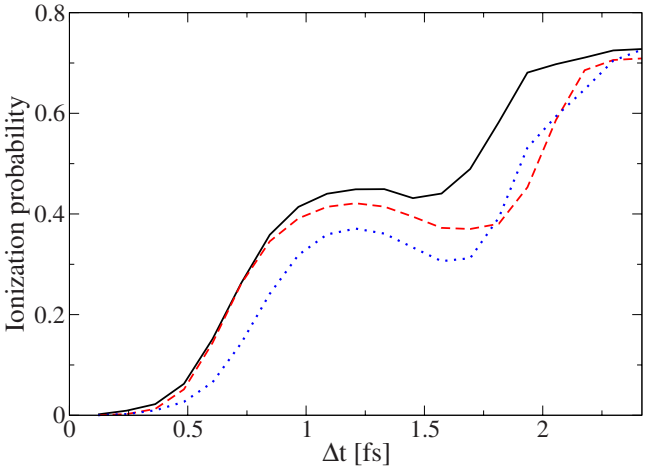

FIG. 8. (Color online) Time dependence of ionization probability for a one-cycle pulse (TDSE results) $\boldsymbol{F}(t)=F_0\sin(\frac{\pi t}{\tau})\hat{\mathbf{z}}$, $0\leqslant t\leqslant 2\tau$. Solid line, $1s$ initial state (result multiplied by 2), peak field strength $F_0=0.1$ a.u. (peak intensity 3.51×10^{14} W/cm^2); dashed line, $2p$ initial state, peak field strength $F_0=0.02$ (peak intensity 1.4×10^{13} W/cm^2); dotted line, $2s$ initial state, peak field strength $F_0=0.02$.

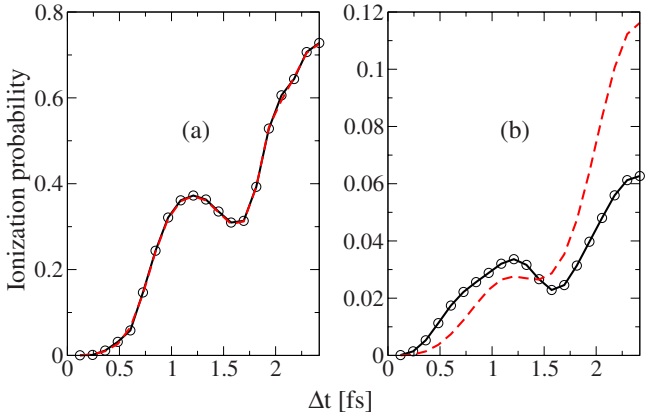

FIG. 9. (Color online) Time dependence of ionization probability for a one-cycle pulse (TDSE results) $\boldsymbol{F}(t)=F_0\sin(\frac{\pi t}{\tau})\hat{\mathbf{z}}$, $0\leqslant t\leqslant 2\tau$, from a coherent superposition of states. (a) Peak field strength $F_0=0.02$ (peak intensity 1.4×10^{13} W/cm^2), comparison of ionization time dependence for $\frac{1}{2}(|2s\rangle+\sqrt{3}|1s\rangle)$ initial state (result multiplied by 4), solid line with open circles, and the case of the $2s$ initial state (dashed line); (b) peak field strength $F_0=0.005$ (peak intensity 8.8×10^{11} W/cm^2), comparison of ionization time dependence for $\frac{1}{2}(|3s\rangle+\sqrt{3}|2s\rangle)$ initial state (result multiplied by 4), solid line with open circles, and the case of the $3s$ initial state (dashed line).

transitions involving the excited states [16]. Indeed, when excited states are not present, such as in the case of the zero-range potential, the recombination from one half-cycle to the other is insignificant [14]. Therefore a theoretical model must include excited states explicitly.

Regarding the relation of binding energy of the initial state to the position of the dip in time, generally the dips occur later in time for a situation where the initial state has smaller binding energy. Initial states with smaller binding energy have larger spatial extension and therefore are more focused in the momentum space. The same can be said for the wave packet of the electrons originating from such an initial state and emitted after the first half-cycle of the field. Assuming that during the interaction the influence of the Coulomb potential is insignificant, the wave packet will tend to recombine at the maximum of the field. This is so because the acquired momentum transfer in the first half-cycle of the field is eliminated at the field maximum of the subsequent half-cycle. This picture is more accurate the larger the intensity. Eventually the wave packet will most likely recombine at the field maximum, resulting in a sharp dip approximately at the instant of the vector potential minimum, as obtained from the numerical calculations in Ref. [9].

We note that here we have restricted ourselves to an analysis at the photon energy of $\omega=0.057$ a.u., corresponding to the widely available laser source of 800 nm. The subcycle ionization probability heavily depends on the relation of the central photon frequency to the characteristic times of the electron in the initial state. The limit of short interaction times compared to the electron characteristic times for the 800-nm and 400-nm pulses corresponds to initial states with binding energy equal to or less than the fourth and third shells of hydrogen, respectively. At such combinations of initial-state binding energies and photon energy, analysis becomes simple. More precisely, there is periodic occurrence of ionization and recombination in time, and therefore at the end of the odd half-cycles of the field, from which the pulse is composed, the ionization probability will exhibit a maximum and minimum at the end of the even half-cycles [27].

As already discussed in Sec. II, in the switch-on type of experiments the effect of the attosecond pulse is to create a coherent superposition of states, which then ionize in the presence of the femtosecond pulse. Therefore, it is instructive to investigate whether the structures in the time dependence of the ionization probability remain in this situation as well. In Fig. 9 two extreme cases of coherent superposition of states are treated: with large, Fig. 9(a), and small, Fig. 9(b), energy separation. Compared with the case of Ne^+ used in the experiment [5] the case in Fig. 9(a) is a larger energy separation and in Fig. 9(b) is smaller. The coherent superpositions are such that in both cases 75% of the population resides in the low-lying state: in Fig. 9(a) we have taken the initial state to be the coherent superposition $\frac{1}{2}(\sqrt{3}\phi_{1s}+\phi_{2s})$ and, in Fig. 9(b), $\frac{1}{2}(\sqrt{3}\phi_{2s}+\phi_{3s})$. In the same figures, dashed lines show the ionization time dependence obtained when only the high-lying state is taken as initial. For large energy separation, as in Fig. 9(a), the low-lying state hardly participates in the dynamics and therefore the ionization curve is identical to the one obtained taking only the high-lying state into account, the factor of 4 being a result of the occupation of the high-lying state in the coherent superposition. However, in the case of Fig. 9(b), the obtained curves in both cases are not identical, reflecting the fact that at such small energy separation the low-lying state actively participates in the dynamics, albeit it cannot alter the absolute values of probabilities significantly. One can conclude that in all cases the dips are present and their occurrence is not connected to the ionization from a coherent superposition of states, in accordance with the observations in Ref. [9].

VI. CONCLUSION

In summary, we considered the time-resolved ionization dynamics in atoms in connection with an xuv-attosecond-pump–near-ir-femtosecond-probe schemes both numerically and analytically. We have identified that the first-order time-dependent perturbation is a unique simple tool for the description of the occupation of bound states and even the time dependence of ionization in the weak-field regime.

At short times there are clear signatures of half-cycle ionization in the time dependence of ionization. At later stages of the pulse, when enough time has passed, the photon picture becomes applicable and the signatures of half-cycle ionization are no longer visible.

We have also considered in detail the structures in the time dependence of ionization, including the rise time and the subsequent dip. The analysis was based on half- and one-cycle responses. For the half-cycle pulse it is shown that even in cases when the tunneling expression gives the exact result at the end of the half-cycle pulse, it is inappropriate to use the tunneling expression to calculate the ionization time dependence *during* the pulse. Instead, one observes a transition from the short-time to the adiabatic limit during the pulse.

For weak fields the ionization probability oscillates in synchrony with the electric field, creating dips at moments of time when the electric field of the pulse is zero. These dips can be very well predicted using FPT. On the other hand, at large amplitudes, where significant ionization occurs during each half-cycle, dips of another type occur and their origin is the recombination of the population ionized from the previous half-cycle into the excited states. These dips occur after the zero-field point, and in cases with large ionization the dips occur very close to the maximum of the electric field of the subsequent half-cycle. Finally, by considering a coherent superposition of states as the initial state, we have shown that the main contribution to structures in the time dependence of ionization stems from the state with the smallest binding energy.

While the present study concentrates on ionization and excitation dynamics in atomic systems, the conclusions we draw are expected to be more generally valid. In particular, the transition from the short-time to the adiabatic limit during the time evolution of the pulse, responsible for the appearance of structures in the time-resolved ionization probability, should be present for any system that can be described by one active electron and a potential—e.g., molecules in the single-active-electron model.

ACKNOWLEDGMENT

This work was supported by the Danish Research Agency (Grant No. 2117-05-0081).

[1] P. M. Paul, E. S. Toma, P. Breger, G. Mullot, F. Auge, Ph. Balcou, H. G. Muller, and P. Agostini, Science **292**, 1689 (2001).
[2] M. Drescher, M. Hentschel, R. Kienberger, G. Tempea, C. Spielmann, G. A. Reider, P. B. Corkum, and F. Krausz, Science **291**, 1923 (2001).
[3] G. Sansone, E. Benedetti, F. Calegari, C. Vozzi, L. Avaldi, R. Flammini, L. Poletto, P. Villoresi, C. Altucci, R. Velotta, Science **314**, 443 (2006).
[4] T. Remetter, P. Johnsson, J. Mauritsson, K. Varju, Y. Ni, F. Lepine, E. Gustafsson, M. Kling, J. Khan, R. Lopez-Martens, Nat. Phys. **2**, 323 (2006).
[5] M. Uiberacker *et al.*, Nature (London) **446**, 627 (2007).
[6] P. Johnsson, J. Mauritsson, T. Remetter, A. L'Huillier, and K. J. Schafer, Phys. Rev. Lett. **99**, 233001 (2007).
[7] G. L. Yudin and M. Yu. Ivanov, Phys. Rev. A **64**, 013409 (2001).
[8] A. K. Kazansky and N. M. Kabachnik, J. Phys. B **40**, F299 (2007).
[9] A. K. Kazansky and N. M. Kabachnik, J. Phys. B **41**, 135601 (2008).
[10] L. B. Madsen and D. Dimitrovski, Phys. Rev. A **78**, 023403 (2008).
[11] O. Smirnova, M. Spanner, and M. Yu. Ivanov, J. Phys. B **39**, S307 (2006).
[12] O. Smirnova, M. Spanner, and M. Yu. Ivanov, Phys. Rev. A **77**, 033407 (2008).
[13] D. Dimitrovski and E. A. Solov'ev, J. Phys. B **39**, 895 (2006).
[14] C. Arendt, D. Dimitrovski, and J. S. Briggs, Phys. Rev. A **76**, 023423 (2007).
[15] R. B. Watkins, W. M. Griffith, M. A. Gatzke, and T. F. Gallagher, Phys. Rev. Lett. **77**, 2424 (1996).
[16] D. Dimitrovski, T. P. Grozdanov, E. A. Solov'ev, and J. S. Briggs, J. Phys. B **36**, 1351 (2003).
[17] T. K. Kjeldsen, L. A. A. Nikolopoulos, and L. B. Madsen, Phys. Rev. A **75**, 063427 (2007); L. A. A. Nikolopoulos, T. K. Kjeldsen, and L. B. Madsen, *ibid.* **75**, 063426 (2007); **76**, 033402 (2007).
[18] L. V. Keldysh, Sov. Phys. JETP **20**, 1307 (1965).
[19] F. H. M. Faisal, J. Phys. B **6**, L89 (1973); H. R. Reiss, Phys. Rev. A **22**, 1786 (1980).
[20] H. A. Bethe and E. E. Salpeter, *Quantum Mechanics of One- and Two-Electron Atoms* (Plenum, New York, 1977).
[21] D. B. Milosević, G. G. Paulus, and W. Becker, Opt. Express **11**, 1418 (2003); S. X. Hu and A. F. Starace, Phys. Rev. A **68**, 043407 (2003).
[22] T. Yamabe, A. Tachibana, and H. J. Silverstone, Phys. Rev. A **16**, 877 (1977).
[23] L. D. Landau and L. M. Lifshitz, *Quantum Mechanics: Non-Relativistic Theory* (Pergamon, Oxford, 1962); B. A. Lippmann and T. F. O'Malley, Phys. Rev. A **2**, 2115 (1970); A. I. Greiser, Sov. Phys. J. **17**, 1225 (1974).
[24] J. S. Briggs, V. I. Savichev, and E. A. Solov'ev, J. Phys. B **33**, 3363 (2000).
[25] D. Bauer and P. Mulser, Phys. Rev. A **59**, 569 (1999).
[26] D. Bauer, D. B. Milosević, and W. Becker, Phys. Rev. A **72**, 023415 (2005); J. Mod. Opt. **53**, 135 (2006).
[27] D. Dimitrovski, E. A. Solovev, and J. S. Briggs, Phys. Rev. A **72**, 043411 (2005).